Supporting information

attached to

Crystal structure of formamidinium–lead-chloride–dimethyl sulfoxide and phase relationship of related crystalline systems

Noriko Saito, Yoshitaka Matsushita, Takeo Ohsawa, Hiroyo Segawa and Naoki Ohashi*

National Institute for Materials Science (NIMS), 1-1 Namiki, Tsukuba, Ibaraki 305-0044, Japan.

*Corresponding author: OHASHI.Naoki@nims.go.jp

S-1 Structure parameters optimization by DFT total energy calculations

Here, the crystal structure of some compounds calculated in this study are shown in **Tables** from **S-I** to **S-VIII**.

In this study, a plane-wave-based pseudo-potential method implemented in CASTEP code,[1] a part of the Materials Studio Package (Dassault Systèmes, Tokyo, Japan), was adopted for optimization of crystal structures based on the density-functional-theory. The norm-conserved pseudopotentials generated by the CASTEP code was used and a generalized gradient approximation optimized for solids (PBESol)[2] was employed as the exchange-correlation functional for self-consistent total energy calculations. The plane-wave cut-off energy was set to 1050 eV and two sampling points on a Monkhorst–Pack grid[3,4] was involved in total energy calculations. Structural optimization was performed with the Broyden–Fletcher–Goldfarb–Shanno scheme.[5]

For $PbCl_2$,[6] CsCl,[7], DMSO,[8] and orthorhombic $CsPbCl_3$,[9] the initial structural models for optimization were constructed refereeing experimentally determined structures. However, some structures, *i.e.* FACl, was purely theoretically determined, as any information about crystal structure of this compound could not be found by the authors. A super-cell model was employed for calculation on $FAPbCl_3$ crystallized in perovskite-type structure in order to describe disordered orientation of FA^+. Particularly, the space group of *Pccn* (D_{2h}) was applied for the model of $FAPbCl_3$ to avoid spontaneous polarization. The initial model for $CsPbCl_3$-DMSO was constructed by simply substituting Cs^+ ion for FA^+ ion in $FAPbCl_3$-DMSO lattice experimentally determined in this study.

S-2 Mulliken charge of elements in $FAPbCl_3$-DMSO

The effective charge of elements in $FAPbCl_3$-DMSO was evaluated by Mulliken charge analysis for the structure optimized by DFT calculation. The result of charge analysis is show in **Table S-IX**.

S-3 Thermal desorption from $FAPbCl_3$-DMSO

Decomposition of $FAPbCl_3$-DMSO at elevated temperature was examined by measuring thermal desorption spectrometry (TDS). The samples, crystalline $FAPbCl_3$-DMSO was set in an ultra-high-vacuum chamber equipped with high temperature stage and quadrupole-mass-spectrometer (QMS). The sample was heated with the high temperature stage from room temperature to 150°C with a constant rump rate and the temperature was hold at 150°C. The desorbed elements and molecules were analyzed with QMS.

Figure S-I shows TDS signal for $FAPbCl_3$-DMSO, particularly the signal profile for m/z=78 and 80. There are two observed profile and one calculated profile. Here, it was assumed that observed signal at m/z=78 is originated in $^{12}C_2{}^{1}H_6{}^{32}S^{16}O$. As the natural abundance of ^{32}S and ^{34}S are 95.029% and 4.218%, respectively, expected signal intensity for $^{12}C_2{}^{1}H_6{}^{34}S^{16}O$ (DMSO) can be calculated from the observed signal intensity for $^{12}C_2{}^{1}H_6{}^{32}S^{16}O$. As the observed and calculated signal intensity for m/z=80 were in good agreement, we can safely identify that m/z=78 and 80 are for $^{12}C_2{}^{1}H_6{}^{32}S^{16}O$ and $^{12}C_2{}^{1}H_6{}^{34}S^{16}O$. Hence, the TDS signal at m/z=80 can be used for discussion on desorption of DMSO.

Figure S-II shows TDS signal for $FAPbCl_3$-DMSO, particularly the signal profile for m/z=35 and 37. Here, it was assumed that m/z=35 and 37 are for ^{35}Cl and ^{37}Cl. As natural abundance of ^{35}Cl and ^{37}Cl are 75.777% and 24.237%, the profile for m/z=35 can be calculated from the observed profile for m/z=37. As shown in the figure, the calculated and observed profile for m/z=35 obviously differ at relatively low temperature range. Hence, the difference between observed and calculated signal are also plotted. Here, it has to be noted that the difference between observed and calculated signal for m/z=35 (purple line) looked very similar to the profile for m/z=78 and 80 shown in Fig. S-I. As another possible assignment for m/z =35 is $^{32}S^{1}H_3$, $^{34}S^{1}H$, and $^{32}S^{2}H^{1}H$, the difference profile can be attributed to those surfer hydride fragments. On the other hand, the observed and calculated profile at m/z=35 are in good agreement at higher temperature, the observed profile for m/z=37 was identified to ^{37}Cl, and that for m/z=37 to S–H fragment at lower temperature and ^{35}Cl fragment at higher temperature. Hence, the signal at m/z=37 can be regarded as the desorption profile for Cl. The critical difference between Cl and CMSO in terms of TDS profile was that desorption of DMSO was completed at T<100°C but Cl continuously desorbed at T>100°C. It is presumable that desorption of Cl at T>100°C is due to gradual evaporation of $FAPbCl_3$ from surface.

Figure S-III shows TDS signal for $FAPbCl_3$-DMSO, particularly the signal profile for m/z=12, 14, 16 and 28. The signal for m/z= 12 and 14 at T<100°C looked very similar to the signal for DMSO shown in Fig. S-I. Hence, signal at m/z=12 and 14, particularly at T<100°C should be identified as ^{12}C and $^{12}C^{1}H_2$ originated in desorption of DMSO. However, the behavior of the signal at m/z=12 and 14 was obviously different from that of DMSO (m/z=80) at higher temperature, T>100°C. As described above, desorption of DMSO was completed at T<100°C. However,

signal intensity for m/z=12 and 14 decreased very slowly even at T>100°C. Hence, origin of the signal at m/z=12 and 14 was not DMSO. The long tail behavior at high temperature was commonly seen for the signal at m/z=16 and 28. Further, behaviors of the signal at m/z=16 and 28 differ from those of DMSO related fragments. Therefore, it is presumable that m/z=16 and 28 were not dominated by desorption of DMSO. Here, it can be assumed that the m/z=16 is for $^{14}N^1H_2$ and m/z=28 for $^{14}N_2$ and/or $^{12}C_2{}^1H_4$. This identification suggests us that FA is remained in the lattice even at T>100°C. As the sample was corrected even after holding at T=150°C, gradual desorption of Cl and FA continued at T>100°C was from the surface and was not due to decomposition.

Figure S-IV shows SEM image of the sample before and after TDS measurement. The crushed $FAPbCl_3$-DMSO crystal (left) was used as specimen for TDS measurement is compared with the residual solid collected after TDS measurement. As mentioned heating in vacuum induced decomposition of $FAPbCl_3$-DMSO by desorption of DMSO. The grains in the residual powder shows porous feature, which was resulting from formation of paths for desorption of DMSO.

References

1. S. J. Clark, M. D. Segall, C. J. Pickard, P. J. Hasnip, M. I. J. Probert, K. Refson and M. C. Payne, First Principles Methods using CASTEP, *Z. Kristallogr.,* 2005, **220**, 567–570.
2. J. P. Perdew, A. Ruzsinszky, G. I. Csonka, O. A. Vydrov, G. E. Scuseria, L. A. Constantin, X. Zhou and K. Burke, Restoring the Density-Gradient Expansion for Exchange in Solids and Surfaces, *Phys. Rev. Lett.*, 2008, **100**, 136406.
3. H. J. Monkhorst and J. D. Pack, Special Points for Brillouin-Zone Integrations, *Phys. Rev.*, 1976, **B13**, 5188-5192.
4. J. D. Pack and H. J. Monkhorst, "Special Points for Brillouin-Zone Integrations"—a Reply, *Phys. Rev.*, 1977, **B 16**, 1748-1749.
5. B. G. Pfrommer, M. Cote, S. G. Louie and M. L. Cohen, Relaxation of Crystals with the Quasi-Newton Method, *J. Comput. Phys.,* 1997, **131**, 233-2401.
6. M. Lumbreras, J. Protas, S. Jebbari, G. J. Dirksen and J. Schoonman, Structure and Ionic Conductivity of Mixed Lead Halides $PbCl_{2x}Br_{2(1-x)}$. II, *Solid State Ionics*, 1986, **20**, 295-304.
7. M. Sist, K. F. F. Fischer, H. Kasai and B. B. Iversen, Low-Temperature Anharmonicity in Cesium Chloride (CsCl), *Angew Chem Int Ed Engl.*, 2017, **56**, 3625-3629.
8. R. Gajda and A. Katrusiak, Electrostatic Matching versus Close-Packing Molecular Arrangement in Compressed Dimethyl Sulfoxide (DMSO) Polymorphs, *J. Phys. Chem.,* 2009, **B113**, 2436–2442.
9. L. Zhang, L. Wang, K. Wang and B. Zou, Pressure-Induced Structural Evolution and Optical Properties of Metal-Halide Perovskite $CsPbCl_3$, *J. Phys. Chem.,* 2018, **C122**, 15220–15225.

Table S-I Crystal structure of $FAPbCl_3$-DMSO under symmetrical restriction with $P2_1/c$.

Monoclinic, $P2_1/c$	
a = 9.7797 Å	α = 90°
b = 14.0003 Å	β = 115.2331°
c = 8.9975 Å	γ = 90°

Fractional atomic coordinates

	x	y	z
Pb	0.16041	0.61248	0.61325
S	0.14901	0.38669	0.77283
O	0.26027	0.46832	0.79576
Cl1	0.46516	0.63439	0.74795
Cl2	0.13419	0.46229	0.39167
Cl3	0.84084	0.23046	0.61889
N1	0.51570	0.60185	0.42568
N2	0.43671	0.60330	0.14195
C1	0.10184	0.39755	0.94288
C2	0.26165	0.28150	0.83640
C3	0.41998	0.62457	0.27536
H1A	0.03088	0.33657	0.94313
H1B	0.03600	0.46385	0.92090
H1C	0.20719	0.40126	1.05666
H2A	0.18597	0.22196	0.83181
H2B	0.35130	0.29202	0.96153
H2C	0.31122	0.26759	0.74932
H1N1	0.61740	0.56820	0.45272
H1N2	0.49167	0.61884	0.52418
H2N1	0.53017	0.56648	0.14703
H2N2	0.35848	0.63033	0.03237
H3	0.31852	0.66441	0.26148

Schematic structure

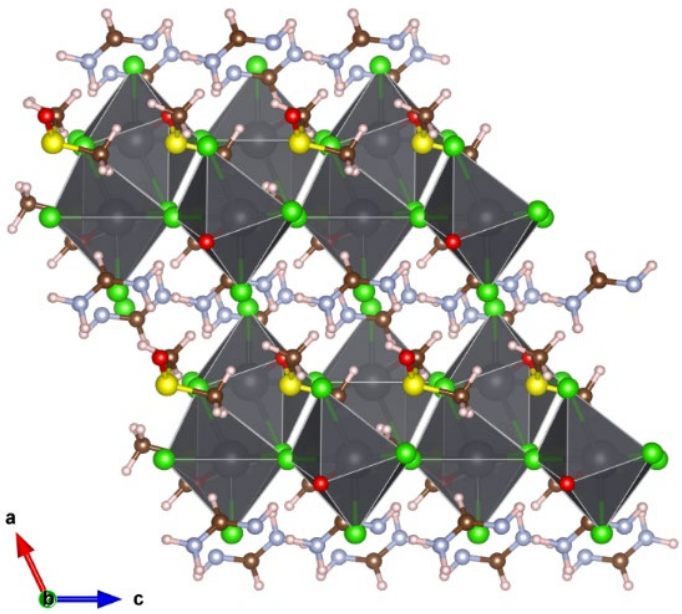

Table S-II Optimized crystal structure of $CsPbCl_3$-DMSO, where Cs^+ was substituted for FA^+ in $FAPbCl_3$-DMSO.

Triclinic, *P*1	
a = 9.5262 Å	*α* = 90.0077°
b = 14.1760 Å	*β* = 114.5148°
c = 8.3379 Å	*γ* = 89.9838°

Fractional atomic coordinates

	x	*y*	*z*
Pb1	0.16419	0.89226	0.11741
Pb2	0.16401	0.60640	0.61724
Pb3	−0.16298	0.10657	0.88312
Pb4	−0.16360	0.39220	0.38301
Cs1	0.39490	0.89796	0.74847
Cs2	0.60624	0.10019	0.25150
Cs3	0.39452	0.60025	0.24805
Cs4	0.60613	0.39900	0.75184
O1	0.22926	0.49301	0.86527
O2	−0.22683	0.99341	0.63504
O3	−0.22897	0.50573	0.13536
O4	0.22774	0.00539	0.36557
S1	0.13443	0.09665	0.31706
S2	0.13554	0.40190	0.81698
S3	−0.13456	0.59656	0.18355
S4	−0.13295	0.90237	0.68345
Cl1	0.47158	0.62886	0.71348
Cl2	0.17734	0.43928	0.43756
Cl3	−0.16569	0.24324	0.63216
Cl4	−0.47066	0.12775	0.78698
Cl5	−0.17630	0.93925	0.06242
Cl6	0.16607	0.74297	0.86841
Cl7	−0.47106	0.37042	0.28722
Cl8	−0.17628	0.55940	0.56306
Cl9	0.16582	0.75538	0.36763
Cl10	0.47193	0.87033	0.21394
Cl11	0.17813	0.05971	0.93862
Cl12	−0.16591	0.25594	0.13146
C1	0.10415	0.37441	1.00797
C2	−0.10152	0.87490	0.49246
C3	−0.26630	0.80942	0.66113
C4	0.10209	0.12408	0.50748
C5	−0.10314	0.62355	−0.00760
C6	−0.26747	0.68983	0.16124
C7	0.26908	0.30898	0.83945
C8	0.26855	0.18930	0.34040
H1	0.21299	0.25715	0.34367
H2	0.37166	0.17767	0.46452
H3	0.04574	0.30568	0.98755
H4	0.02812	0.42826	1.02411
H5	0.21623	0.37358	0.12355
H7	0.21335	0.24126	0.84301
H8	0.37251	0.32041	0.96331
H9	0.29395	0.31151	0.72211
H10	0.29385	0.18657	0.22337

H11	0.21372	0.12408	0.62371
H12	−0.04333	0.80610	0.51252
H13	−0.02535	0.92867	0.47643
H14	−0.21361	0.87427	0.37689
H15	−0.21029	0.74170	0.65809
H16	−0.36965	0.82070	0.53712
H17	−0.29133	0.81221	0.77835
H18	−0.04367	0.69190	0.01263
H19	−0.02809	0.56909	−0.02394
H20	−0.21532	0.62483	0.87697
H21	−0.21134	0.75742	0.15785
H22	−0.37098	0.67857	0.03739
H23	−0.29235	0.68734	0.27858
H24	0.04475	0.19315	0.48766
H25	0.02484	0.07062	0.52218

Schematic structure

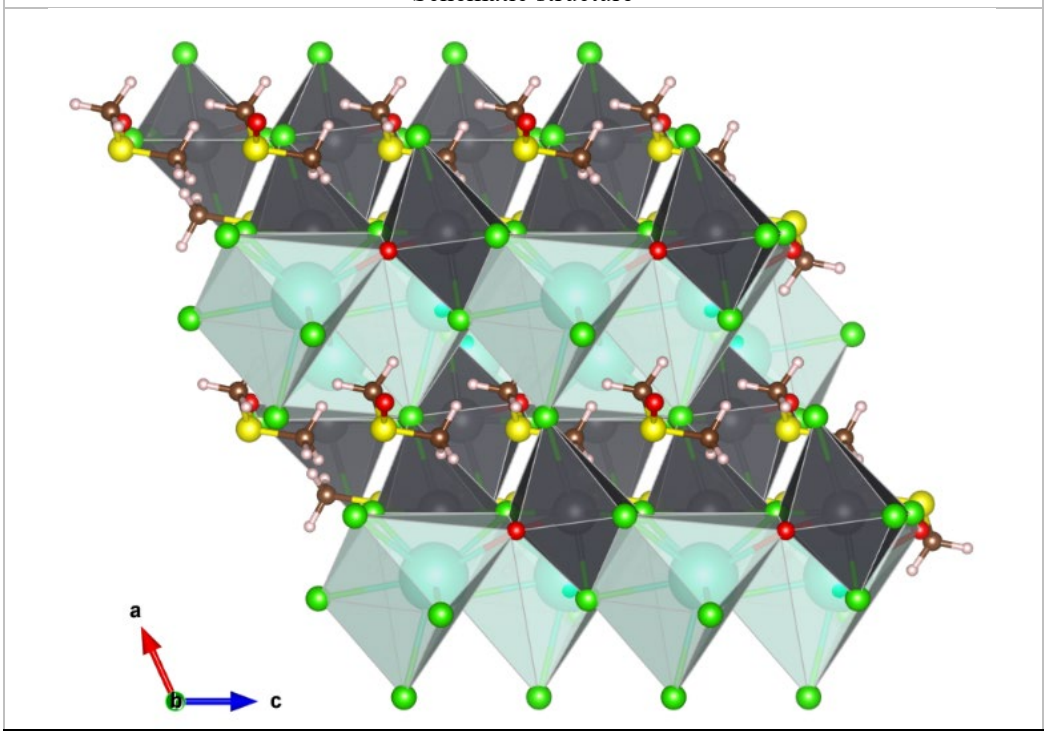

Table S-III Optimized crystal structure of $CsPbCl_3$ crystallized in orthorhombic symmetry.

Orthorhombic, *Pbnm*	
a = 7.8565 Å	α = 90°
b = 7.9536 Å	β = 90°
c = 11.0290 Å	γ = 90°

Fractional atomic coordinates

	x	y	z
Pb	0.50000	0.00000	0.00000
Cs	0.98032	0.95097	0.25000
Cl1	0.10169	0.53544	0.25000
Cl2	0.78432	0.21676	0.04335

Schematic structure

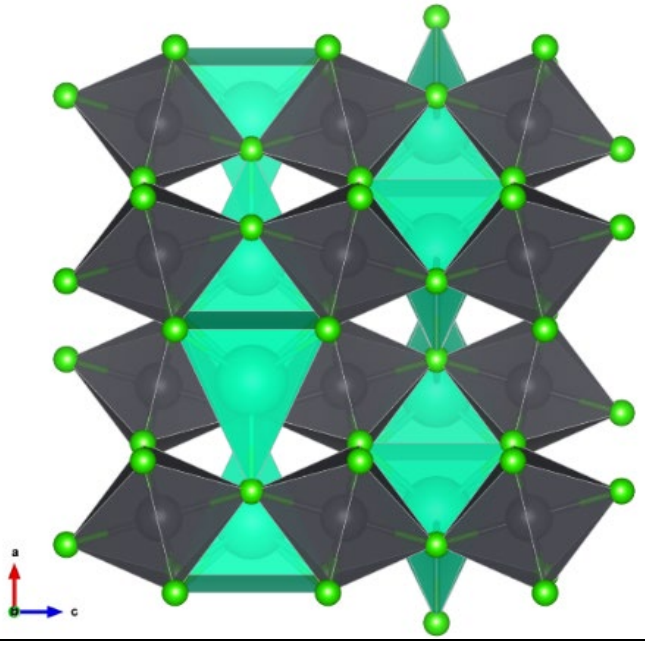

Table S-IV Optimized crystal structure of $FAPbCl_3$, super-cell, under structural restriction of *Pccn* symmetry to avoid spontaneous polarization.

Orthorhombic, *Pccn*	
a = 11.7054 Å	α = 90°
b = 11.4073 Å	β = 90°
c = 12.4175 Å	γ = 90°

Fractional atomic coordinates

	x	y	z
Pb1	0.25000	0.25000	0.48049
Pb2	−0.25000	0.25000	0.48900
Cl1	0.25000	0.25000	−0.23638
Cl2	0.00247	0.24968	−0.01175
Cl3	0.23949	0.49805	−0.04501
Cl4	−0.25000	0.25000	0.19433
C	−0.48006	0.50086	−0.25167
N1	−0.52755	0.41277	−0.30304
N2	−0.52174	0.54661	−0.16315
H1	−0.48496	0.61753	−0.12603
H2	−0.40104	0.53720	−0.28565
H3	−0.59869	0.51964	−0.13007
H4	−0.49153	0.37880	−0.37175
H5	−0.59991	0.37166	−0.27466

Schematic structure

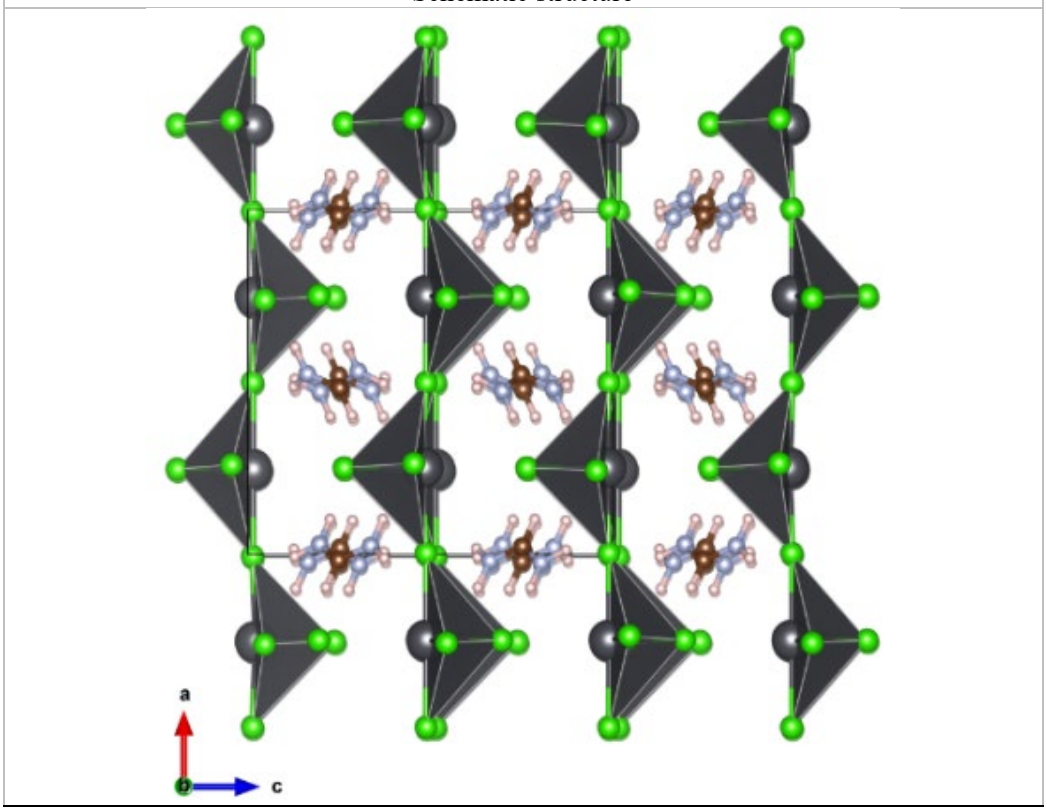

Table S-V Optimized crystal structure of $PbCl_2$.

Orthorhombic, *Pnam*	
a = 7.5287 Å	α = 90°
b = 9.0631 Å	β = 90°
c = 4.4805 Å	γ = 90°

Fractional atomic coordinates

	x	y	z
Cl1	0.85842	0.07895	0.25000
Cl2	0.48318	0.84096	0.25000
Pb	0.26279	0.09440	0.25000

Schematic structure

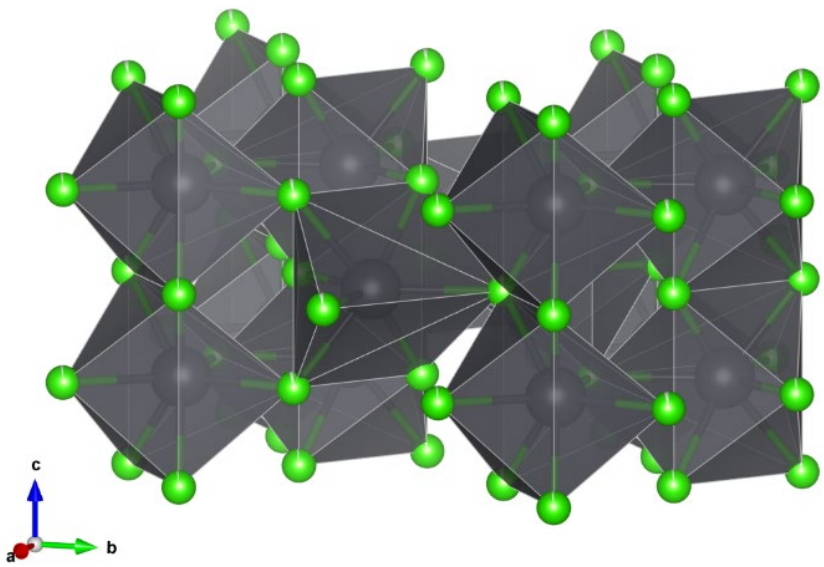

Table S-VI Optimized crystal structure of CsCl

Cubic, *Pm*3*m*	
a = 4.0726 Å	α = 90°
b= 4.0726 Å	β = 90°
c = 4.0726 Å	γ = 90°

Fractional atomic coordinates

	x	*y*	*z*
Cs	0.00000	0.00000	0.00000
Cl	0.50000	0.50000	0.50000

Schematic structure

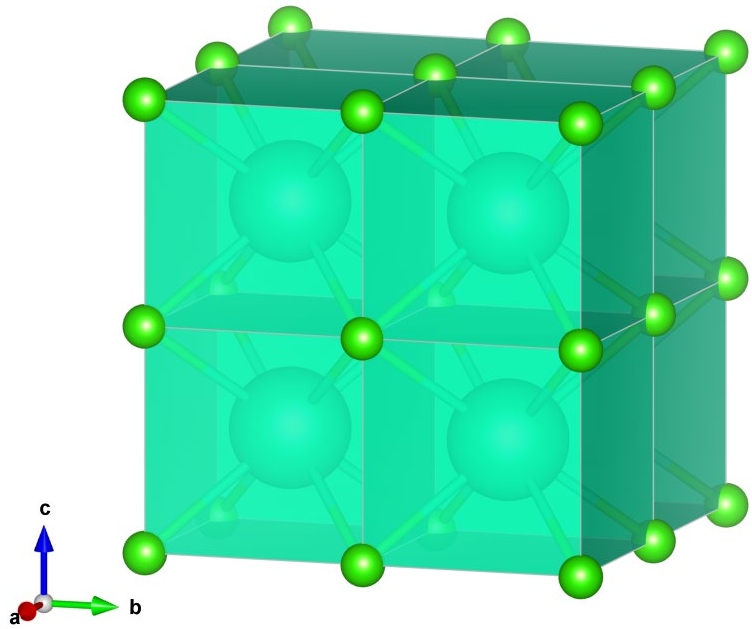

Table S-VII Optimized crystal structure of FACl.

Monoclinic, $P2_1/c$	
a = 9.6732 Å	α = 90°
b = 8.3902 Å	β = 45.9126°
c = 9.4058 Å	γ = 90°

Fractional atomic coordinates

	x	y	z
Cl	1.25051	0.40686	0.16259
C	0.67335	0.27707	0.56568
N1	0.80767	0.35239	0.54157
N2	0.48831	0.27968	0.72661
H1	0.71884	0.20223	0.44321
H1A	0.95013	0.34893	0.40719
H1B	0.77545	0.42752	0.64960
H2A	0.39705	0.21848	0.72351
H2B	0.42838	0.33744	0.85679

Schematic structure

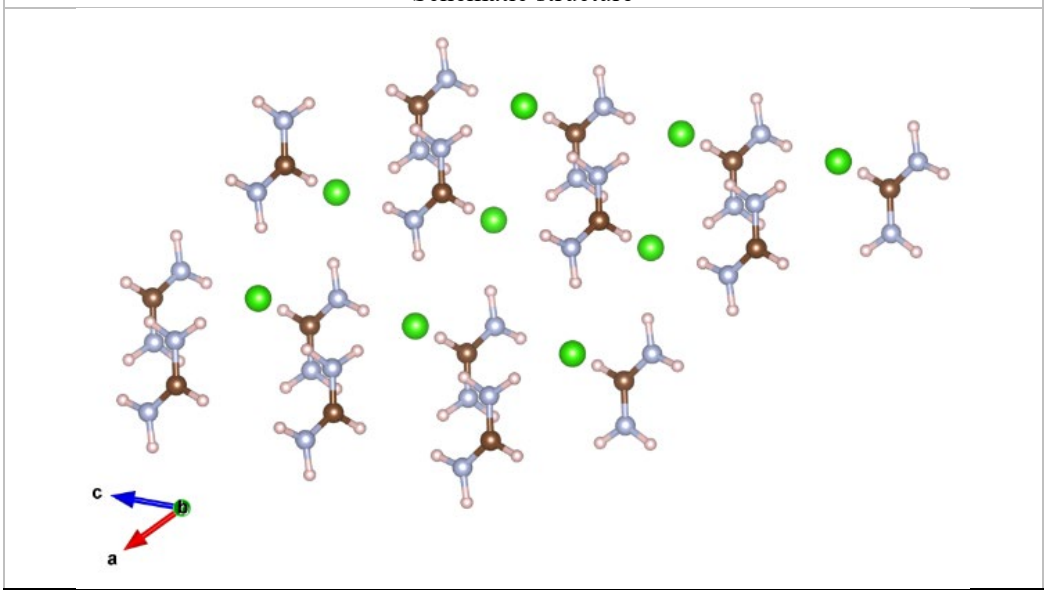

Table S-VIII Optimized crystal structure of crystalline DMSO.

Monoclinic, $P2_1/c$	
a = 5.2160 Å	α = 90°
b = 7.2517 Å	β = 94.2831°
c = 11.3532 Å	γ = 90°

Fractional atomic coordinates

	x	y	z
S	0.32445	0.09735	0.29765
O	0.61174	0.09197	0.32298
C1	0.19417	−0.09124	0.37547
C2	0.20490	0.27933	0.38541
H1A	0.26824	−0.08734	0.46914
H1B	0.25229	−0.21811	0.33107
H1C	−0.01695	−0.07649	0.36654
H2A	0.28368	0.26344	0.47752
H2B	0.26599	0.40996	0.34673
H2C	−0.00664	0.26906	0.37871

Schematic structure

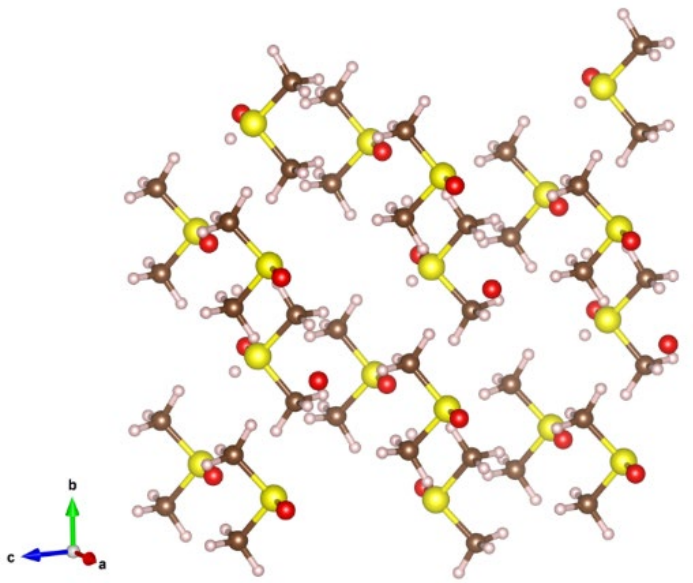

Table S-IX Mulliken charge of elements in $FAPbCl_3$-DMSO

Element	Charge / e
H	0.31
C	-0.54
N	-0.72
O	-0.93
S	1.12
Cl	-0.58
Pb	1.16

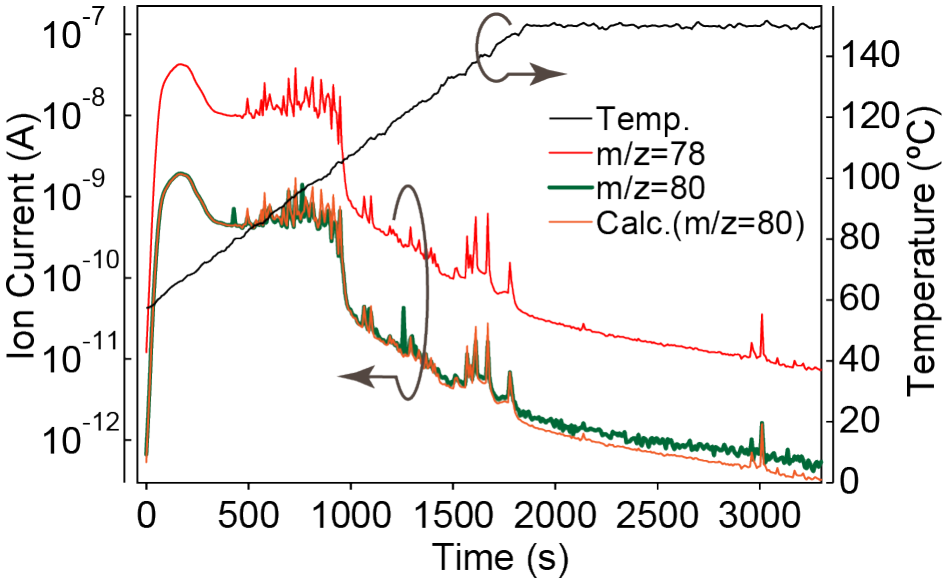

Figure S-I TDS profile of $FAPbCl_3$-DMSO, particularly the fragment with m/z=78 and 80. One of two profiles for m/z=80 was experimentally observed (green line) and the other (red line) was calculated by assuming that observed signal at m/z=78 and calculated signal at m/z=80 correspond to $^{12}C_2{}^{1}H_6{}^{32}S^{16}O$ and $^{12}C_2{}^{1}H_6{}^{34}S^{16}O$.

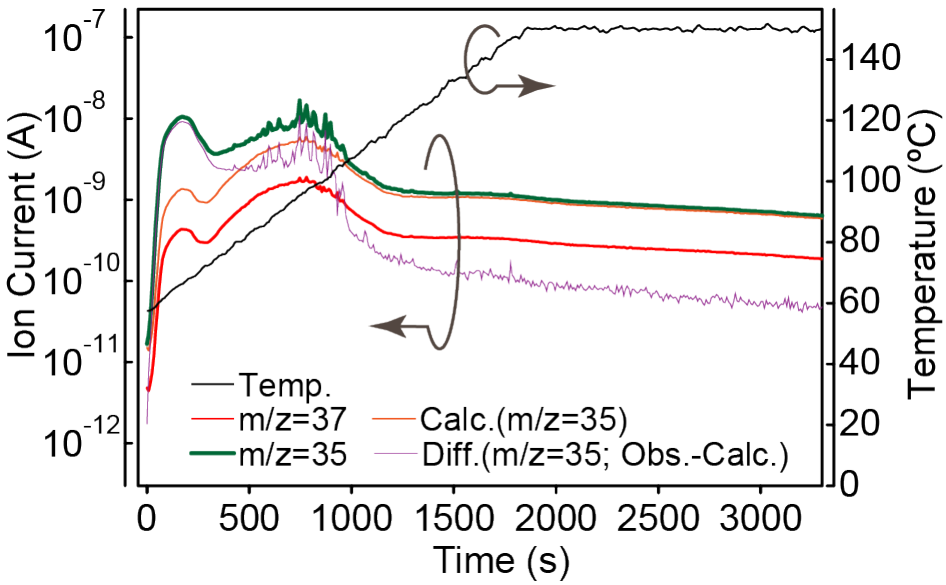

Figure S-II TDS profile of $FAPbCl_3$-DMSO, particularly the fragment with m/z=35 and 37. There are two profiles for m/z=35. One was observed (green line) and the other (orange line) was calculated by assuming the fragment with m/z=35 and 37 were for ^{35}Cl and ^{37}Cl. In addition, the difference between observed and calculated profile for m/z=35 (purple line) is shown.

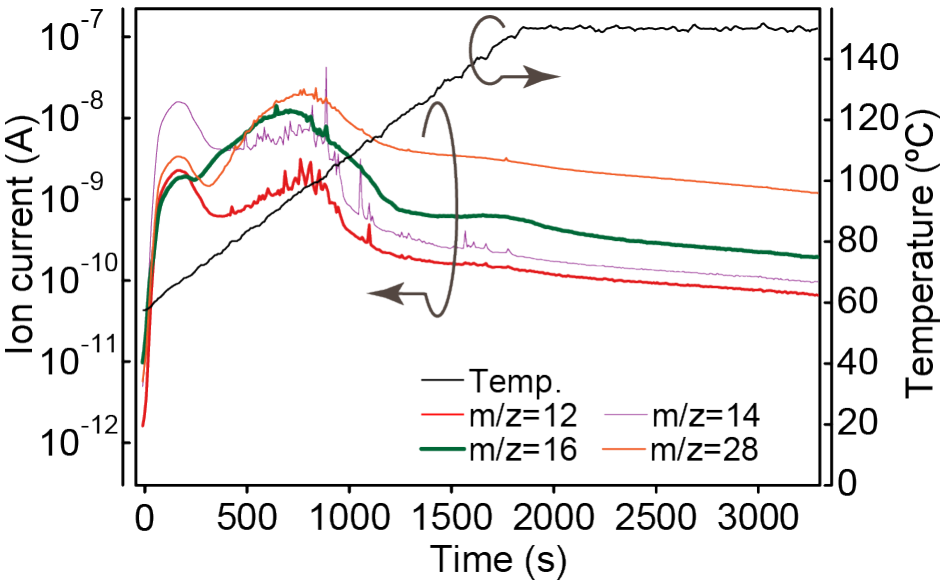

Figure S-III TDS profile of $FAPbCl_3$-DMSO, particularly observed behavior for the fragment with m/z=12, 14, 16, and 28.

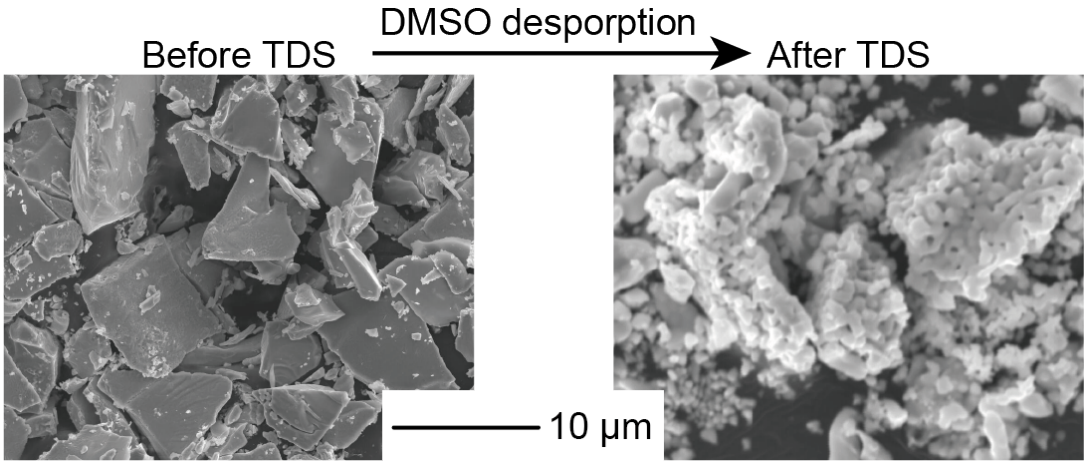

Figure S-IV SEM image of crushed $FAPbCl_3$-DMSO crystal used for TDS measurement (left) and the residual solid after TDS measurement.